

Numerical Investigation of the Nonlinear Cyclic Behavior of Special Reinforcing Bars for Precast Concrete Frames with Hybrid Connections

Andrei Faur^{*1}, Călin Mircea²

^{1,2} *Technical University of Cluj-Napoca, Faculty of Civil Engineering. 15 C Daicoviciu Str., 400020, Cluj-Napoca, Romania*

Received 15 September 2012; Accepted 5 November 2012

Abstract

Hybrid connections are a viable solution for erecting precast concrete frame structures in seismic areas. Such type of connections makes use of unbounded post-tensioned strands and partially unbounded mild steel rebars, also known as special reinforcing bars, in order to assemble the precast frame units. The paper presents a study about the nonlinear cyclic behavior of the special reinforcing bars along their unbounded length. Such type of reinforcement serves as the major energy dissipater for the precast concrete hybrid frame system and therefore, is subjected to severe plastic deformations during earthquakes. One uniaxial steel model is used to obtain the cyclic stress-strain curves following an elongation-controlled loading case scenario. Previous test observations and results were considered to establish the probable compression and tensile strain limits. A parametric study was done in order to compensate the lack of test data needed to calibrate the steel model. The results found through several numerical simulations reveal an unique cyclic behavior of the special reinforcement that clarifies some aspects regarding the cyclic behavior of the entire connection.

Rezumat

Îmbinările hibride sunt o soluție viabilă pentru realizarea structurilor prefabricate din beton armat în zone seismice. Aceste tipuri de conexiuni folosesc toroane post-tensionate neaderente și armături de oțel parțial neaderente, cunoscute și sub denumirea de armături speciale, pentru asamblarea elementelor prefabricate. Această lucrare prezintă un studiu despre comportarea ciclică neliniară întâlnită pe lungimea de neaderență a barelor de armătură specială. Aceste tipuri de armături au rol de disipatori de energie pentru îmbinările de tip hibrid și, prin urmare, în timpul cutremurelor sunt supuse la deformații plastice severe. În urma unui scenariu de încărcare-descărcare controlat în deformații de tip axial, un model uniaxial folosit la modelarea barelor de oțel este utilizat pentru a obține curbele ciclice forță-deplasare. Rezultatele și observațiile unor teste experimentale ulterioare au fost folosite pentru a stabili limitele deformațiilor care sunt probabile să se producă atât la întindere, cât și la compresiune. Un studiu parametric a fost necesar pentru a compensa lipsa datelor experimentale folosite pentru calibrarea modelului uniaxial. Rezultatele obținute în urma mai multor simulări numerice prezintă o comportare unică la solicitări ciclice a armăturii speciale, care clarifică unele aspecte legate de comportarea ciclică a întregii îmbinări.

Keywords: uniaxial steel model, cyclic behavior, special reinforcement, hybrid frame connections,

^{*}Corresponding author: Tel./ Fax.: +40 264 40 15 45
E-mail address: Andrei.FAUR@dst.utcluj.ro

hardening rules, numerical simulation.

1. Introduction

The mild steel reinforcement used to assemble the precast frame units of hybrid frame systems is called special reinforcement (SR), because the rebars are intentionally unbounded over a short length, in order to guide and to be able to sustain large axial deformations without fracturing. The rebars are also individually introduced into steel ducts, of which are bonded with fiber reinforced grouts. Along with the post-tensioned (PT) strands, the SR ensures the bending capacity of the connection, and separately, has the major role to dissipate the seismic energy induced to the connection.

The transition from the un-deformed state to the deformed state when the hybrid connection is subjected to an enforced lateral displacement is represented in Fig. 1. As shown, a gap opens at the beam-column interface, which causes the PT steel and the SR bars to elongate. Due to the post-tensioning effect, the connection re-centers itself and forces the SR to return to its original length. When the lateral load is applied in the other direction, the same SR bars, that were previously stretched, are now compressed along with the concrete located in the compression region. This loading-unloading sequence repeats with every lateral displacement applied to the connection.

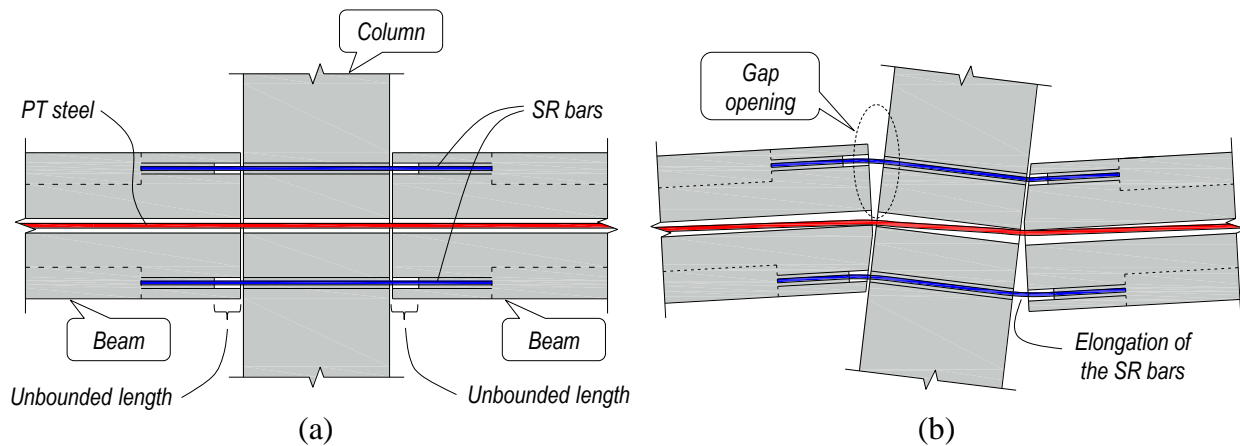


Figure 1. Hybrid connection detail under both un-deformed (a) and deformed state (b).

The percentage of special reinforcement influences the cyclic behavior of hybrid connections. As stated by Ozden & Ertas [1], the optimum percentage corresponds to a contribution of 30% to the connection's bending moment capacity. The rest up to 70% is provided by the PT steel. Lower SR percentages will finally lead to a bilinear spring behavior, while the larger ones will finally cause a monolithic connection behavior [1].

Recent studies [2] have shown through numerical simulations of a tested beam-to-column sub-assembly that the unbounded length is also responsible for the connection's response. By varying the unbounded length and considering an optimum amount of special reinforcement (by the same criteria stated by Ozden & Ertas [1]), it was found that a length of 7.5 to 10 bar diameters should not be bonded in order to achieve a typical hybrid connection behavior.

2. Research significance

The existent studies claim an optimum SR contribution of around 30% to the overall bending capacity of the connection. For this reason and considering that the lateral resistance is provided mostly by the PT steel, it is of great interest to determine to which extent the strain-hardening of the SR influences the entire connection response to cyclic loadings. The implications of such a result

ε_s^{norm} – the normalized strain value, defined in Eq. (3);

$$\varepsilon_s^{norm} = \frac{\varepsilon - \varepsilon_r^{(n-1)}}{\varepsilon_y^{(n)} - \varepsilon_r^{(n-1)}} \quad (3)$$

b – the hardening ratio, defined in Eq. (4);

$$b = E_{sh} / E_s \quad (4)$$

and $R_n(\xi_n)$ – curvature parameter, defined in Eq. (4).

$$R_n(\xi_n) = R_0 - \frac{A_1 \cdot \xi_n}{A_2 + \xi_n} \quad (5)$$

The terms from Eq (2) to Eq (5) have the following meanings: ε – current strain; σ – the stress corresponding to ε ; $\varepsilon_y^{(n)}$, $\sigma_y^{(n)}$ – the yield strain and stress of the current n -th half-cycle; $\varepsilon_r^{(n-1)}$, $\sigma_r^{(n-1)}$ – the strain and stress associated with the last inversion point; E_{sh} – the hardening stiffness (i.e., tangent of the hardening branch); E_s – the initial tangent modulus (i.e., modulus of elasticity); R_0 , A_1 , A_2 – material constants; ξ_n – plastic excursion, defined as the distance between the inversion and yield points of the last half-cycle (Eq. (6)).

$$\xi_n = \varepsilon_r^{(n-1)} - \varepsilon_y^{(n-1)} \quad (6)$$

In essence, each half-cycle represents the curved transition from one tangent line of slope E_s to an asymptote line of slope E_{sh} . The Baushinger effect is considered through the $R_n(\xi_n)$ curvature parameter that is actually the transition radius between the tangent and the asymptote line. As seen from Fig. 2 and Eq. (6), $R_n(\xi_n)$ varies with respect to the current plastic excursion ξ_n . In other words, the Baushinger effect for the current half-cycle depends on the previous loading history.

Eq. (1) to Eq. (6) define the Menegotto-Pinto model. The Monti-Nuti model brings in addition four hardening rules in order to assess for a more realistic cyclic behavior. Two of this rules, referred as *isotropic* and *kinematic hardening rules* [3], evaluate the yield stress for the current n -th half-cycle. The plastic path followed during the whole loading history is taken into account through the *memory rule*, while the rotation of the asymptote of slope E_{sh} is considered through the *saturation rule* [3]. Someway or another, all hardening rules account for the plastic excursion followed by the material during all the half-cycles performed.

If the isotropic, kinematic and memory rule are considered simultaneously, the yield stress of the n -th half-cycle (i.e., the current half-cycle) is evaluated through Eq. (7).

$$\sigma_y^n = \sigma_y^{(0)} \cdot \text{sign}(-\xi_n) + \left[P \sum_{i=1}^{n-1} bE\xi_i + (1-P) \left[\sum_{i=1}^{n-1} |bE\gamma_i| \cdot \text{sign}(\Phi_i) \right] \cdot \text{sign}(-\xi_n) \right] \quad (7)$$

where:

P – weighing coefficient;

γ_i – additional plastic excursion, evaluated through Eq. (8) and Eq. (9):

$$\gamma_i = \begin{cases} (|\xi_{i-1}| - \xi_{max}) \cdot \text{sign}(\xi_{i-1}), & \text{if: } |\xi_{i-1}| > \xi_{max} \\ 0, & \text{if: } |\xi_{i-1}| \leq \xi_{max} \end{cases} \quad (8)$$

$$\xi_{max} = \max(|\varepsilon_r^{(i)} - \varepsilon_y^{(i)}|); \quad i = \{0 \dots n-2\} \quad (9)$$

Φ_i – plastic work, defined in Eq. (10).

$$\Phi_i = \frac{1}{2} \left(\sigma_r^{(i-1)} - \sigma_y^{(i-1)} \right) \xi_i \quad (10)$$

For each half-cycle, the saturation rule considers a different value for the hardening ratio b_n which is updated through Eq. (11).

$$b_n = b \cdot e^{\left(bE \sum_{i=1}^{n-1} \gamma_i \right) / (-0.5\sigma_y^{(0)})} \quad (11)$$

The Monti-Nuti model is completely defined through Eq. (1) ÷ Eq. (11), but for evaluation of the curvature parameter $R_n(\xi_n)$, the model accounts for the maximum plastic excursion reached. Thus, Eq. (5) becomes:

$$R_n(\xi_n) = R_0 - \frac{A_1 \cdot \xi_{max}}{A_2 + \xi_{max}} \quad (12)$$

3.2 Special reinforcement characteristics and cyclic loading scenario

The SR used for the numerical simulation is considered to be part of a hybrid frame connection which is designed to withstand a relative drift of 2.5%. At this level, the connection should encounter only minor damages if designed properly. This implies that no spalling of the concrete cover and no fracture of the SR occurs. Also, it is assumed that the PT steel maintains its restoring force and still has the ability to push the tensioned SR bars down to the compression state permitted by the surrounding concrete area.

Such a behavior has been observed in previous experimental programs also. Several 1/3 scale frame-to-column sub-assemblies with hybrid connections were tested at NIST (*National Institute of Standards and Technology*) [5], while later, a 60% scale five-story precast/prestressed concrete building was exposed to a simulated seismic loading during the PRESSS (*Precast Seismic Structural Systems*) research program [6]. More recently, several 1/2 scale specimens similar to those tested at NIST, but having different percentages of SR, were tested by Ozden and Ertes [1], and also an experimental program was conducted at INCERC (*National Institute for Research & Development in Construction and Economy of Construction*) Cluj-Napoca Branch, where a full-scale specimen was subjected to a displacement controlled cyclic loading sequence up to a relative drift of 2.5% [7]. The hybrid connection performed as expected under all these tests, at least for relative drifts lower than 2.5%, and it suffered only minimum residual displacements and minimum damages of the beam end concrete cover.

The numerical simulation is performed for the SR of the specimen tested at INCERC Cluj-Napoca. Given the above-mentioned considerations, the maximum compression strain limit is taken as the nominal ultimate strain of the surrounding concrete (i.e., equal to 3.5‰ for C25/30 concrete class), while the maximum tension strain limit is taken as the strain corresponding to the tensile strength of the reinforcement. The used steel has the yield strength of 345MPa and the tensile strength of 510MPa. During the test, the maximum gap opening measured at the location of the SR was about 12mm. For a 90mm unbounded length plus the additional unbounded length resulting from strain penetration, it is assumed that the special reinforcement achieved a maximum strain of about 1%. The value corresponds to the maximum drift encountered by the hybrid frame sub-assembly.

A total of 28 complete cycles were considered in the numerical simulation. The target elongations were gradually increased for each cycle until they reached the maximum strain limits. Due to the post-tensioning effect, the SR elongations are guided to follow directly the path between two opposite target strain limits (i.e., no other inversion points are considered elsewhere along the loading-unloading path).

3.3 Numerical implementation aspects

The Monti-Nuti steel model was coded in Python [8], which is a high-level programming language suitable for numerical simulations. The Numpy [9] extension module was also used to benefit of the *ndarray* (i.e., a multidimensional array object) data type.

The target strain limits, the plastic excursion values, and the yield and reversal points coordinates (i.e., $\epsilon_y, \sigma_y, \epsilon_r, \sigma_r$ values) were organized using one-dimensional arrays of *ndarray* data type. In this manner, the whole loading history was stored with minimum memory resources. After each load reversal, the arrays are updated with the newly obtained values. For example, the array that stores the inversion point strain values $[\epsilon_r]$ is concatenated with the newly encountered reversal strain $[\epsilon_r^{(n)}]$ (see Eq. (13)):

$$[\epsilon_r] = [\epsilon_r^{(0)} \quad \epsilon_r^{(1)} \quad \dots \quad \epsilon_r^{(i)} \quad \dots \quad \epsilon_r^{(n-1)}] \parallel [\epsilon_r^{(n)}] = [\epsilon_r^{(0)} \quad \epsilon_r^{(1)} \quad \dots \quad \epsilon_r^{(i)} \quad \dots \quad \epsilon_r^{(n-1)} \quad \epsilon_r^{(n)}] \quad (13)$$

The same procedure applies to all arrays except for the target strain limits array which is a fix-length data type.

4. Numerical analysis results

Material constants R_0, A_1 and A_2 were found through a calibration process. The goal was to obtain the idealized bilinear curve of the steel used for the SR. Every time, the weighing coefficient P was taken as zero ($P = 0$). The values for which the curve generated with the Monti-Nuti steel model is identical to the material idealized bilinear curve are:

$$R_0 = 20.0 \quad A_1 = 19.0 \quad A_2 = 0.3 \quad (14)$$

The lack of test data for calibrating the weighing coefficient P led to a parametric study on which the whole range of possible values (i.e., $P = [0 \dots 1]$) were considered in increments of 0.10. Thus, a total of 10 numerical simulations were performed to capture the cyclic behavior of the SR, three of them (i.e., for $P = 0; P = 0.5$ and $P = 1$) being presented in figures: Fig. 3 – for $P = 0$; Fig. 4 – for $P = 0.5$; Fig. 5 – for $P = 1$. The notations *sig* and *sig_ENV* represent the cyclic stress-strain curves and the envelope curve, respectively, while steel idealized bilinear curve is depicted with dash line.

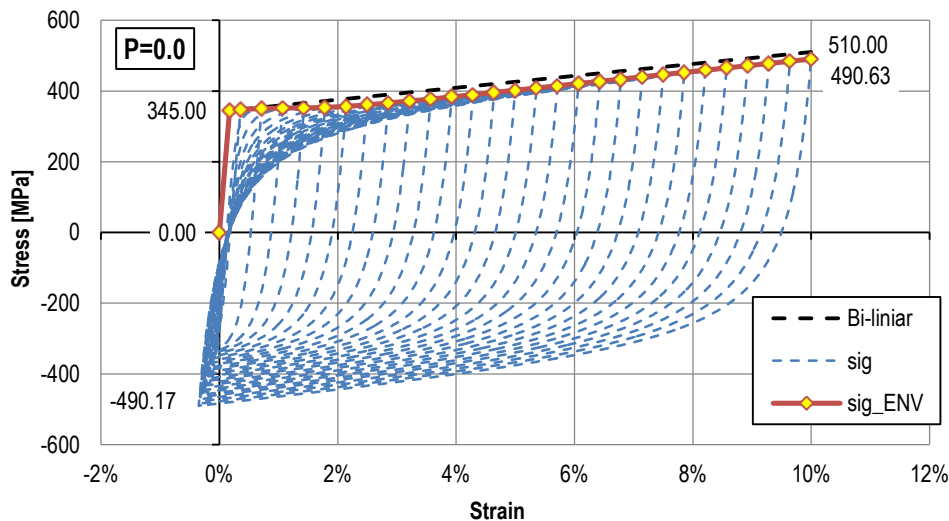


Figure 3. Numerical results using the Monti-Nuti model when $P=0$.

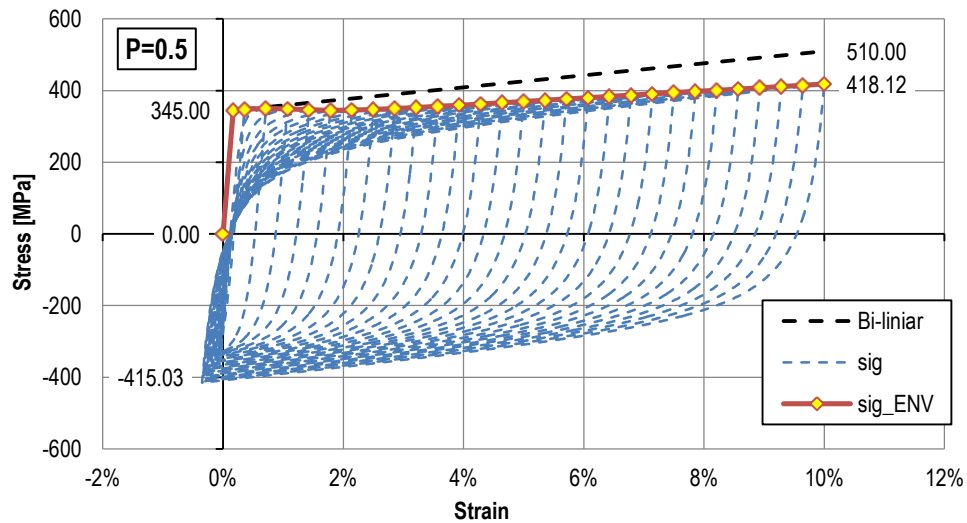


Figure 4. Numerical results using the Monti-Nuti model when $P=0.5$.

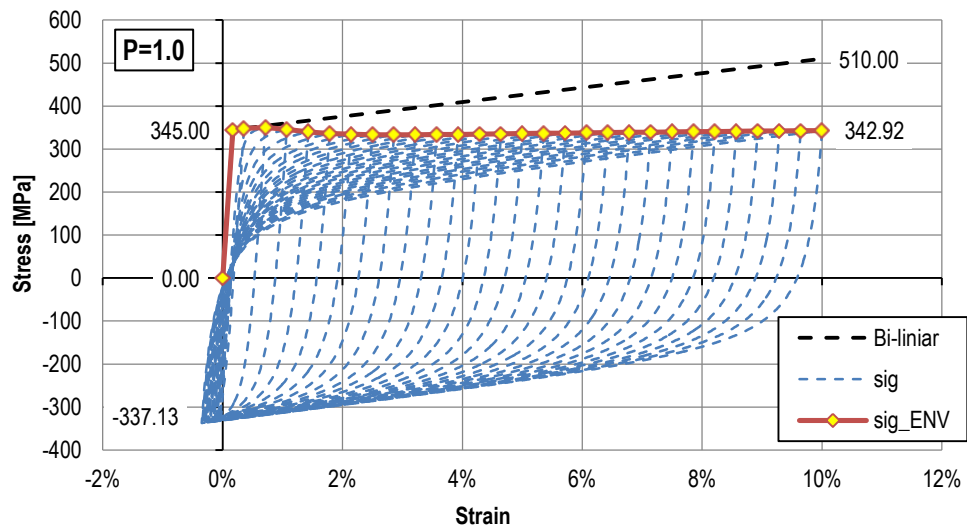


Figure 5. Numerical results using the Monti-Nuti model when $P=1$.

As observed, if P approaches 1.0, the envelope curve moves away from the bilinear curve, while for $P=0$, the envelope and the bilinear curves almost overlap, the differences between their maximum stresses being lower than 4% (see Table 1). This behavior can be explained by Eq. (7). The first sum represents the kinematic rule and is multiplied by P , while the second sum represents the mixed isotropic and memory rule and is multiplied by $(1-P)$ [3]. Therefore, no kinematic hardening is considered if $P=0$ and no isotropic hardening is taken into account if $P=1$.

Table 1: Comparison between bilinear curve and numeric envelope curves

Result provenance	Maximum stress	Minimum stress	Aria of the last cycle
	[MPa]	[MPa]	[MPa×%]
Steel ideal bilinear curve	510.00	0.00	-
Monti-Nuti model ($P=0.0$)	490.63	-490.17	69.41
Monti-Nuti model ($P=0.5$)	418.12	-415.03	58.25
Monti-Nuti model ($P=1.0$)	342.92	-337.13	46.06

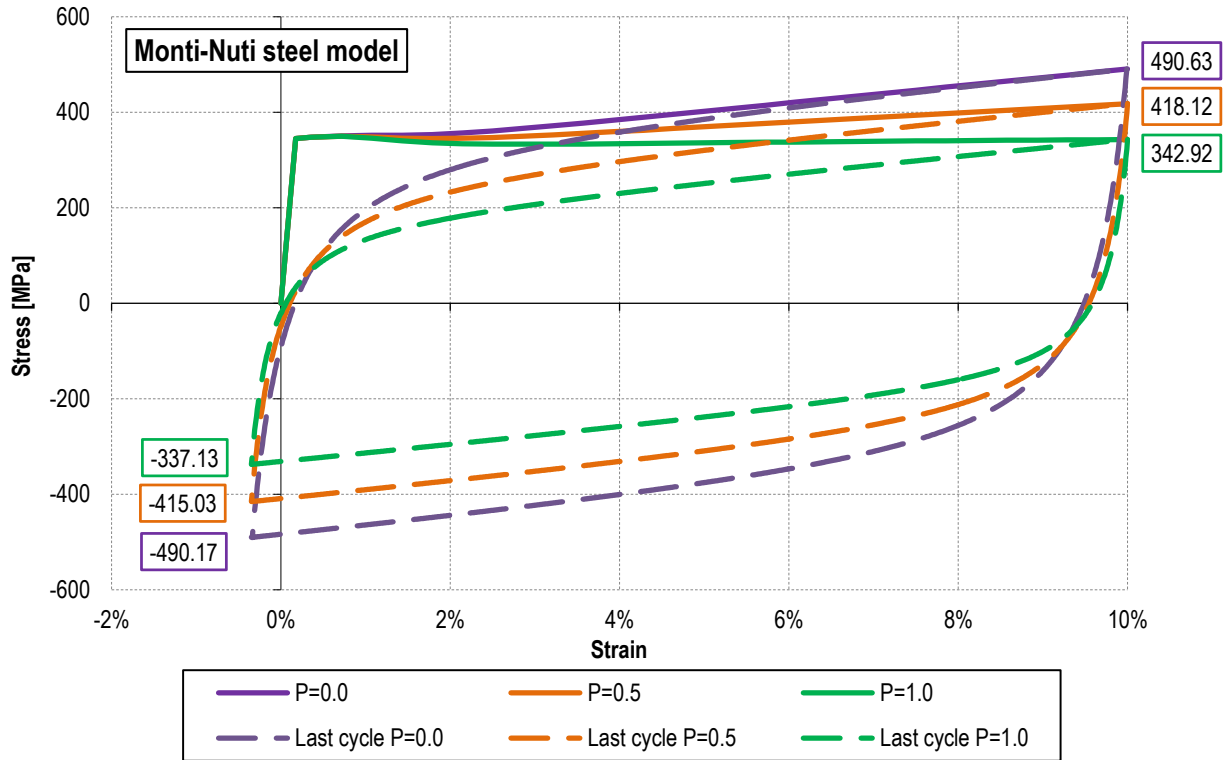


Figure 6. Comparison of envelope and last cycle curves for different P values

The results presented in Fig. 3 to Fig. 6 and Table 1 are a clear evidence that the cyclic behavior of the SR is characterized more by a “softening” tendency, depending on the material’s predisposition to kinematic or isotropic strain-hardening. Moreover, the last cycle areas tend to decrease as the isotropic strain-hardening becomes less pronounced (i.e., P approaches 1.0), the differences being higher than 33% between the cases where $P=0$ and $P=1$.

In a theoretical case, where the compression and tension strain limits are equal, the Monti-Nuti model with $P=0$ generates the curves from Fig. 7. It can be seen that the “hardening” tendency is

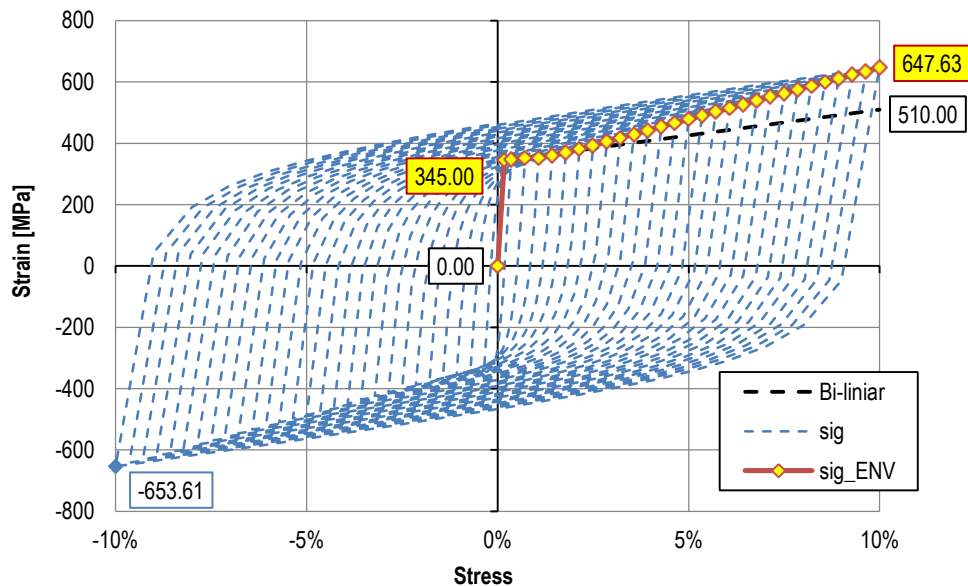


Figure 7. Numerical results for symmetric strain limits when $P=0$

highly pronounced, the differences between the bilinear and envelope curves at their maximum strains being higher than 20%. This behavior is explained by the fact that the material (i.e., the SR bar) is subjected with every half-cycle to a plastic excursion which is almost twice as higher than the plastic excursion normally encountered by the SR. In other words, the stress will probably exceed those predicted by the idealized bilinear curve if large deformations occur in both directions (i.e., in tension and compression). Otherwise, if the compression strains are limited to 3.5‰, the envelope curve of the tension stress will definitely be below the idealized bilinear curve, whatever the material hardening properties are.

5. Effect of cyclic behavior of the SR on the overall behavior of the connection

The numerical analysis revealed that the SR undergoes no strain-hardening as long as no spalling of concrete cover occurs. In fact, the tendency seems to be of strain-softening (i.e., the stress decreases with increasing strain), which is straight-related to the isotropic hardening property of the material. In addition, if an optimum contribution of the SR to the overall bending capacity of the connection is considered, it is possible to encounter similarities between the monotonic force-displacement/moment-rotation curve and the hysteresis envelope curve of the same connection. This implies that the cyclic behavior of the SR is not significantly affecting the cyclic behavior of the entire connection.

Even though such a behavior has been observed in previous studies, it has never been explained. Pampanin et al. [10] and Balica [11] managed to capture the moment-rotation curves of two specimens that were tested at NIST (i.e., the M-P-Z4 and O-P-Z4 specimens [5]) using the Monolithic Beam Analogy (MBA) procedure [10]. Ozden & Ertas [12] followed the same MBA procedure to obtain the moment-rotation curves of four specimens with different percentages of SR. In all three studies the results were sufficiently accurate to predict the hysteresis envelope curves, even if no cyclic analyses were performed and no strain-hardening/softening effect was considered for the SR.

The influence of the SR strain-softening on the overall behavior of the connection can be considered in design by estimating the probable stress encountered by the SR when the connection reaches the design displacement. Thus, the ACI T1.2-03 [13] guidelines were applied to determine the probable flexural strength (M_{pr}) at the beam-column interface of the hybrid connection specimen referred to in [2]. All four maximum stress values mentioned in Table 1 were taken as tensile strength for the SR (f_u). The probable flexural strength associated with a design drift of 2.5% was estimated for each of these cases and the results are shown in Table 2, where M_s and M_{prs} represent the contribution of SR and PT steel to M_{pr} , respectively. As seen, the differences between the maximum and minimum probable flexural strength are less than 10%, even though the tensile strength for the SR varies up to 30%. Also, the contribution of the SR to the overall bending capacity of the connection decreases by $\approx 27\%$ (i.e., from 27.9% to 20.41%). This implies that the SR strain-softening can be ignored in predicting the probable flexural strength at the beam-column interface, but a lower contribution to the overall bending capacity of the connection is recommended to be taken into account.

Table 2: Estimation of probable flexural strength for several SR tensile strength values

P	f_u	M_s	M_{prs}	M_{pr}
[-]	[MPa]	[kNm]	[kNm]	[kNm]
-	510.00	49.64	128.33	177.97
0.0	490.63	47.74	128.46	176.20
0.5	418.12	40.62	128.95	169.56
1.0	342.92	33.20	129.45	162.65

6. Conclusions

A numerical analysis was performed in order to study the cyclic behavior of the special reinforcement used for hybrid precast/prestressed concrete frame systems. Only the behavior of the unbounded region was investigated, of which the cyclic stress-strain curves were found with the use of the Monti-Nuti steel model. The numerical results offer a clear view about the strain-hardening/softening property of the special reinforcement. At least till spalling of concrete cover occurs, the compression strains of the SR are limited to the strains encountered by the surrounding concrete area, and no strain-hardening takes place. A strain-softening behavior is observed instead, which gets more pronounced as the isotropic hardening is less important. Of course, the hardening property of the material needed to calibrate the Monti-Nuti steel model should be determined by tests, but in absence, the performed parametric study reveals that the stresses encountered by the SR will certainly be lower than those predicted through the idealized bilinear curve. Therefore, if the steel constitutive law is taken as an idealized stress-strain curve and the cyclic behavior is neglected, the tensile stresses encountered by the SR can be overestimated, especially for certain type of rebars with no isotropic hardening property.

Despite the above-mentioned considerations, a decrease of the SR envelope curve does not seem to significantly affect the overall bending capacity of the connection. To prove this statement, observations were made about the similarity between the monotonic and the envelope moment-rotation curves encountered in previous studies. In fact, it was observed that the monotonic moment-rotation curve behaves as an envelope for the moment-rotation hysteresis curves. Although never explained, it is considered that the cause of this similarity relies just in the lack of the SR strain-hardening effect, as proved by the results of the performed numerical simulation. Thus, it is sufficiently accurate to consider an idealized stress-strain behavior for the SR, when performing monotonic or cyclic analyses of the whole hybrid connection system.

For design considerations, there is no need to estimate the cyclic behavior of the SR, because there are no significant changes in the overall bending capacity of the connection, and the same idealized stress-strain curve is sufficiently enough to define the constitutive law of the material.

Acknowledgements

This paper was supported by the project „Doctoral studies in engineering sciences for developing the knowledge based society-SIDOC” contract no. POSDRU/88/1.5/S/60078, project co-funded from European Social Fund through Sectorial Operational Program Human Resources 2007-2013.

7. References

- [1] Ozden S, Ertas O. Behavior of Unbonded, Post-Tensioned, Precast Concrete Connections with Different Percentages of Mild Steel Reinforcement. *PCI Journal*, **Vol. March-April**, pp. 32–44, 2007.
- [2] Faur A, Mircea C. Research on Self-Centring Ability of Hybrid Frame Connections. In: *Proc. Taller, Longer, Lighter – Meeting growing demand with limited resources*, 35th Annual Symposium of IABSE / 52nd Annual Symposium of IASS / 6th International Conference on Space Structures, London, September, 2011.
- [3] Monti BG, Nuti C. Nonlinear cyclic behavior of reinforcing bars including buckling. *Journal of Structural Engineering*, **Vol. 118**(12), pp. 3268–3284, 1993.
- [4] Menegotto M, Pinto PE. Methods of Analysis of Cyclically Loaded R.C. Plane Frames Including Changes and Non-Elastic Behavior of Elements under Combined Normal Force and Bending. In: *Proc., IABSE Symposium of Resistance and Ultimate Deformability of Structures Acted on by Well- Defined Repeated Loads*, International Association of Bridge and Structural Engineering, Lisbon, Portugal, pp.

15–22, 1973.

- [5] Stone WC, Cheok GS, Stanton JF. Performance of Hybrid Moment-Resisting Precast Beam-Column Concrete Connections Subjected to Cyclic Loading. *ACI Structural Journal*, **Vol. 91(2)**, pp. 229–249, 1995.
- [6] Priestly MJN, Sritharan S, Conley JR, Pampanin S. Preliminary Results and Conclusions From the PRESSS Five-Story Precast Concrete Test Building. *PCI Journal*, **Vol. November-December**, pp. 42–67, 1999.
- [7] Faur A, Mircea C. Hybrid connections – the sustainable approach for prefabricated frame structures. In: *Proceedings of Concrete Solutions*, 4th International Conference on Concrete Repair, Grantham M, Mechtcherine V, Schneck U, editors. CRC Press, pp. 227-233, 2011.
- [8] <http://www.python.org/doc/>
- [9] <http://docs.scipy.org/doc/>
- [10] Pampanin S, Priestley NJM, Sritharan S. Analytical modelling of the seismic behaviour of precast concrete frames designed with ductile connections. *Journal of Earthquake Engineering*, **Vol. 5(3)**, pp. 329–365, 2001.
- [11] Balica NA. *Contributions on improving the theory and practice of reinforced and prestressed concrete buildings*. PhD Thesis, Technical University of Civil Engineering Bucharest, 2010. (in Romanian).
- [12] Ozden S, Ertas O. Modeling of pre-cast concrete hybrid connections by considering the residual deformations. *International Journal of the Physical Sciences*, **Vol. 5(June)**, pp. 781–792, 2010.
- [13] ACI Innovation Task Group 1 and Collaborators. *Special Hybrid Moment Frames Composed of Discretely Jointed Precast and Post-Tensioned Concrete Members (ACI T1.2-03) and Commentary (ACI T1.2R-03)*, American Concrete Institute, Farmington Hills, Mich., 2003.